

Functional Characterization of Spliceosomal Introns and Identification of U2, U4, and U5 snRNAs in the Deep-Branching Eukaryote *Entamoeba histolytica*^{∇†}

Carrie A. Davis, Michael P. S. Brown, and Upinder Singh*

Departments of Microbiology and Immunology and Internal Medicine, Stanford University School of Medicine, Stanford, California 94305-5124

Received 27 February 2007/Accepted 17 April 2007

Pre-mRNA splicing is essential to ensure accurate expression of many genes in eukaryotic organisms. In *Entamoeba histolytica*, a deep-branching eukaryote, approximately 30% of the annotated genes are predicted to contain introns; however, the accuracy of these predictions has not been tested. In this study, we mined an expressed sequence tag (EST) library representing 7% of amoebic genes and found evidence supporting splicing of 60% of the testable intron predictions, the majority of which contain a GUUUGU 5' splice site and a UAG 3' splice site. Additionally, we identified several splice site misannotations, evidence for the existence of 30 novel introns in previously annotated genes, and identified novel genes through uncovering their spliced ESTs. Finally, we provided molecular evidence for the *E. histolytica* U2, U4, and U5 snRNAs. These data lay the foundation for further dissection of the role of RNA processing in *E. histolytica* gene expression.

Eukaryotic genes are often expressed as discontinuous units requiring the removal of intervening RNA sequences (introns) in order to discern their reading frames and ensure their accurate expression. The pre-mRNA-splicing reaction partners are brought into proximity through dynamic rearrangements of the spliceosome, a RNP complex composed of numerous snRNPs and five noncoding snRNAs: U1, U2, U4, U5, and U6 (18, 27). The precise splice sites are characterized by conserved sequence elements.

Entamoeba histolytica infects an estimated 500 million people annually (41). Cysts are ingested in food and water contaminated with fecal matter and excyst into the disease-causing trophozoite in the small intestine. In most people, this results in asymptomatic colonization and reencystation with no subsequent pathology. However, 50 million of those infected each year develop invasive disease (bloody diarrhea or liver abscesses) (41). How *E. histolytica* regulates gene expression during host invasion, encystation, excystation, and trophozoite vegetative growth is largely unknown.

Prior to completion of the *E. histolytica* genome sequence, only a few introns had been reported (24, 33, 34, 40). Based on these limited data, the consensus amoebic 5' and 3' splice sites (5', GUUUGU; 3', UAG) and the lack of a well-conserved branch point consensus were described (40) and incorporated into the computational gene finders used for genome annotation (24). Given that only a few examples of introns had ever previously been uncovered, it was surprising that the genome-sequencing project revealed 3,188 introns in the 9,938 predicted genes (24). Correct intron removal is therefore a neces-

sity for the accurate expression of at least a third of the presently annotated *E. histolytica* genes. However, the vast majority of these intron predictions lacked molecular validation. The absence of a systematic test of splice site predictions and splicing in this organism presents a significant barrier to our ability to understand its genome structure and the role of RNA processing in amoebic gene regulation.

In this study, we computationally mined an *E. histolytica* expressed sequence tag (EST) library for hallmarks of splicing. The questions we sought to address were (i) how accurate are the current intron predictions and (ii) how complete is our understanding of splicing in this organism. We compared the intron predictions to the processing patterns deduced from EST analysis, mined the ESTs for novel introns, and used covariance models to computationally identify *E. histolytica* snRNAs. We found evidence supporting the splicing of several predicted introns and identified several splice site misannotations, novel introns in annotated genes, and novel intron-containing genes. In addition, we identified EST evidence for intron retention and provided molecular evidence for U2, U4, and U5 snRNAs. These data are the result of the largest-scale test of splicing in this organism to date and form the basis for dissecting the interplay between the spliceosome and other cellular machinery involved in amoebic-gene regulation.

MATERIALS AND METHODS

***E. histolytica* EST library and data sets.** The *E. histolytica* EST library was created from pooled total RNA (from parasites in the mid-log and stationary phases and from a mouse model of amoebic colitis) (Barbara Mann, personal communication). The datasets containing the intron predictions, EST sequences, and gene predictions were downloaded from The Institute for Genomic Research (<http://www.tigr.org/tdb/e2k1/eha1/>).

Computational mapping of ESTs to the genome scaffolds. In order to determine which genomic loci were likely to encode the ESTs, we aligned the EST sequences to the genome sequence data, using the BLAT alignment program (with the version 30 default parameters) (20). Per the default parameters, there were no restrictions on the size of the gap or the amount of 5' and 3' overlap between the ESTs and the genomic sequence. Because each EST should be

* Corresponding author. Mailing address: Department of Medicine, Division of Infectious Diseases, S-143 Grant Building, 300 Pasteur Drive, Stanford, CA 94305. Phone: (650) 723-4045. Fax: (650) 724-3892. E-mail: usingh@stanford.edu.

† Supplemental material for this article may be found at <http://ec.asm.org/>.

[∇] Published ahead of print on 27 April 2007.

nearly identical to the corresponding genomic region (some mismatch was allowed for sequencing errors), we considered alignments that had $\geq 98\%$ sequence identity between the genomic regions and the full-length EST transcript (matches of $>0.98 \times \text{QuerySize}$).

Computational mining of the EST alignments for introns. In order to identify possible introns, we computed the coordinates of unaligned gap regions (i.e., the putative introns) from the BLAT alignments described above. The EST gap coordinates were computationally compared to the 3,188 predicted intron coordinates determined from the genome sequence project (24). If the EST gap coordinates matched the coordinates of a predicted intron, we counted this intron as “spliced as predicted” (see Table S1 in the supplemental material). If the EST gap coordinates did not match the predicted intron, we counted that intron as “spliced but at coordinates other than that which are predicted” (Table 1). If the EST gap coordinates did not map to a region known to contain an intron or gene, we deemed that intron “novel.” If no ESTs mapped to a region containing a predicted intron, we deemed that intron prediction “untestable” and did not consider it further. If only ungapped ESTs mapped to a region containing a predicted intron, we deemed that intron “not spliced as predicted” (see Table S2 in the supplemental material).

Computational identification of snRNAs. We computationally identified the U2 and U4 spliceosomal RNAs using a combination of Hidden Markov models (HMMs) and stochastic context-free grammars (SCFGs), techniques that search for conservation in the primary sequence and secondary structures between a query sequence and a training set (3, 11, 23, 36). U2 and U4 in the Rfam database Release 7.0 were used to train the above programs (14, 15). The majority of the genome sequence was filtered out, using HMMs (default parameters, version 2.3.2). The remainder of the genome sequence with the greatest similarity to known U2 and U4 snRNAs was further scored, using an SCFG (internal package) against the models obtained from Rfam (default parameters, version 0.7). In order to identify U5 snRNA, we downloaded all 235 full sequences of U5 from the Rfam database. We used BLAT (standard parameters, version 30) to align each of these sequences against the full *E. histolytica* genome sequence.

***E. histolytica* cell culture, RNA, and DNA isolation.** *E. histolytica* strain HM-1:IMSS was grown axenically in Trypticase-yeast extract-iron-serum (TYI-S-33) medium (9, 26). Trophozoites were grown to log phase, and total RNA was isolated, using Trizol reagent. Genomic DNA was isolated as indicated by Ali et al. (1).

RT-PCR and Northern blot analysis. One microgram of total RNA was treated with DNase I and incubated with 0.5 μg of oligo(dT)₁₅ for 10 min at 95°C, and reverse transcription and cDNA amplification were performed as by Ehrenkauf et al. (12). The PCR products were electrophoresed on a 6% native acrylamide gel and stained with ethidium bromide. The cDNA PCR products were cloned into a TOPO-TA vector (Invitrogen) and sequenced, and splicing of the intron was determined based on its absence from the cDNA. For Northern blot analysis, 10 μg of total RNA from *E. histolytica* HM-1:IMSS trophozoites was electrophoresed on a 6% acrylamide-7 M urea gel along with a radiolabeled 10-base-pair marker (Invitrogen), transferred onto a Hybond-N⁺ (Amersham) nylon membrane, and cross-linked, using a Stratilinker. Oligonucleotide probes (see Table S3 in the supplemental material) were prepared and used to probe the membrane as described by Davis and Ares (7).

Nucleotide sequence accession numbers. The following sequences have been deposited in GenBank under the numbers indicated: U2 snRNA, BK006130; U4 snRNA, BK006131; and U5 snRNA, BK006132.

RESULTS AND DISCUSSION

***E. histolytica* intron predictions.** The *E. histolytica* genome sequence was completed in 2005 and led to a list of 3,188 putative introns in 9,938 predicted genes (24). This is a substantial number of introns compared to the paucity of introns in the related protists *Giardia lamblia* and *Trichomonas vaginalis*, suggesting that splicing plays a greater role in amoebic-gene regulation (4, 32, 35, 38). In order to gather a global view of the predicted introns, we determined their sizes and their positions with respect to the start codon and the nucleotide frequencies at the 5' and 3' splice donors. Distribution analysis of the predicted *E. histolytica* intron sizes indicated that the vast majority are small, ~40 nucleotides in length (Fig. 1A). This is consistent with previous reports of small introns in *E.*

^a Data for eight intron-containing genes for which the intron prediction did not match the EST data are shown.

TABLE 1. *E. histolytica* intron splice site misannotations^a

Representative EST	Transcript	GenBank accession no.	Predicted function	Predicted sequence at indicated splicing site:		Predicted coordinates	Predicted size	BLAT-EST sequence at indicated splicing site:		BLAT-EST coordinates	BLAT-EST size	No. of unique ESTs
				5'	3'			5'	3'			
EHAG374TR	6.m000476	ELA51573.1	Hypothetical protein	GUUUUU	GAG	122713-123030	317	GUUUUU	UAG	122735-122797	62	1
EHA0181TR	18.m00295	ELA50710.1	Hypothetical protein	GUUUUU	AAG	16364-16517	153	GUUUUU	UAG	16351-16463	112	66
EHAAB92TF	88.m00175	ELA47893.1	Hypothetical protein	GUUUUG	GAG	56505-57006	501	GUUUUG	UAG	56507-56681	174	10
EHAES297TR	50.m00171	ELA49178.1	Vesicular transport	GUUUGA	UAG	22303-22390	87	GUUUUU	UAG	22293-22368	75	1
EHCAC267TR	42.m00212	ELA49475.1	S6 Ribosomal protein	GUUAUG	UAG	76818-76880	62	GUUAUG	UAG	76814-76870	56	3
EHCAC267TR	42.m00214	ELA49453.1	S6 Ribosomal protein	GUUAUG	UAG	86245-86307	62	GUUAUG	UAG	86241-86296	56	3
EHCAC267TR	1066.m00001	ELA44245.1	S6 Ribosomal protein	GUCCAU	AAG	270-365	95	GUUAUG	UAG	280-335	56	3
EHAES83TR	350.m00049	ELA43647.1	Rab family GTPase	GUUAUU	UAG	6630-6679	50	GUUUUU	UAG	6625-6679	54	3
EHAES83TR	350.m00049	ELA43647.1	Rab family GTPase	GUUUUU	UAG	6442-6562	121	GUUUUU	UAG	6442-6503	61	3
EHAES83TR	350.m00049	ELA43647.1	Rab family GTPase	GUUUUU	UAG	6442-6562	121	GUUUUU	UAG	6513-6563	50	3

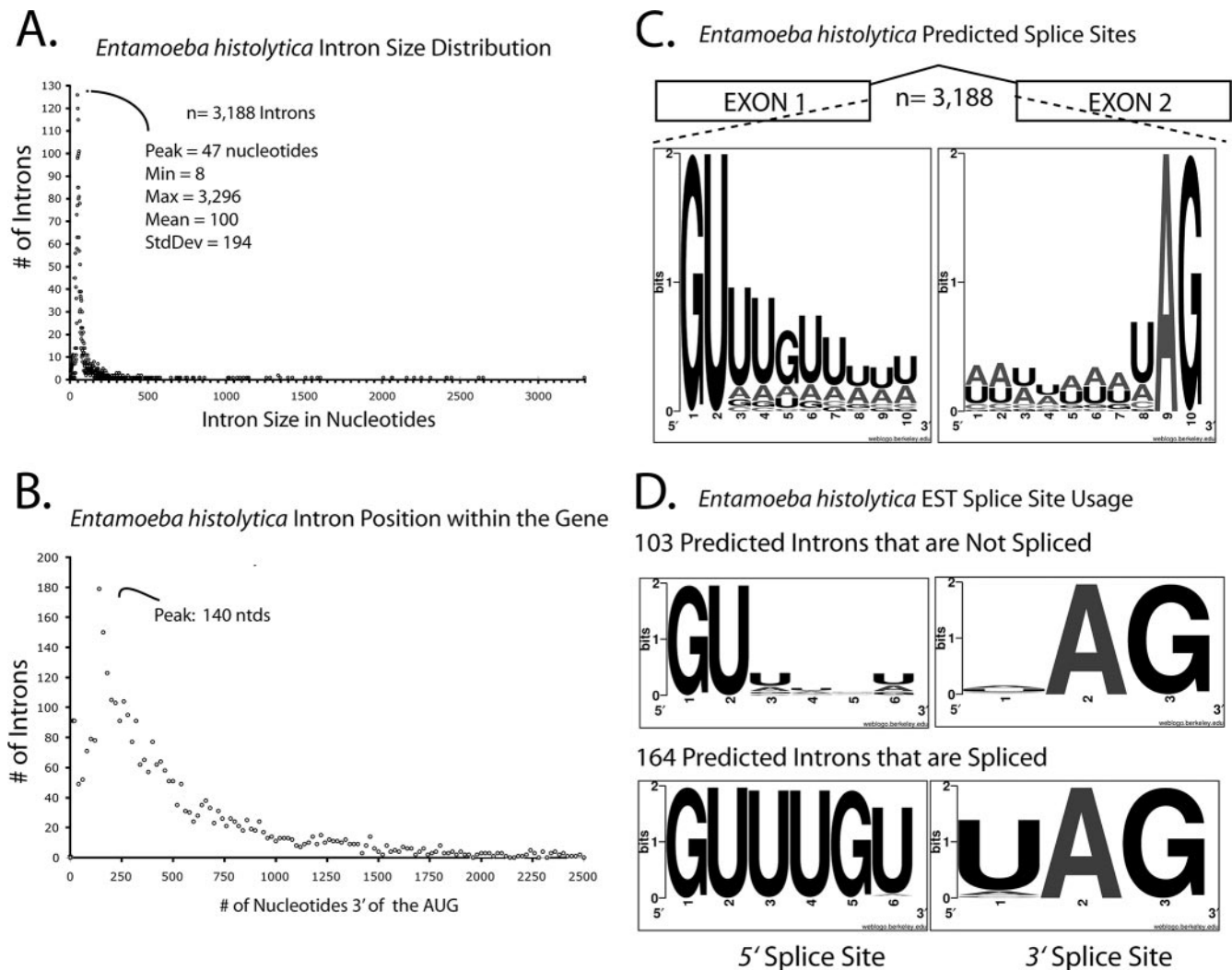


FIG. 1. *E. histolytica* intron attributes. (A) Histogram showing distribution of 3,188 predicted *E. histolytica* intron sizes. The majority of introns are ~40 nucleotides. Note that the x-axis bin size is 1 and that only the major units (50 nucleotides) are depicted. (B) Histogram showing distribution of the distance from the predicted AUG (start codon) to the 5' splice site for each of the 3,188 predicted introns. Note that the x-axis bin size is 5. (C) Sequence LOGO plot illustrating the relative frequency of nucleotide usage for the first 10 nucleotides (extended 5' splice site) and the last 10 nucleotides (extended 3' splice site) for each of the 3,188 predicted introns. (D) Sequence LOGO plot of the first six nucleotides and last three nucleotides of the introns that are spliced as predicted in the ESTs (lower panel) or not spliced as predicted (upper panel).

histolytica (33, 39, 40) and comparable to intron sizes from the single-cell parasites *T. vaginalis* and *G. lamblia* (4, 32, 35, 38). We noticed that 35 of the predicted *E. histolytica* introns are smaller than 23 nucleotides. Although spliceosomal introns as small as 23 nucleotides have been validated in the ciliated *Paramecium* (42), the 23-nucleotide intron size may reflect a lower limit on the geometric constraints for snRNA binding and lariat formation; thus, we concluded that these introns are likely not real (see Table S2 in the supplemental material). Finally, we found that in *E. histolytica*, the highest proportion of introns are located over the 5' end of the transcript length (Fig. 1B), a feature commonly found in intron-sparse genomes (29).

Analyses of the predicted splice sites indicate that the primary 5' splice site is composed of GUUUGU and the 3' splice site is UAG (Fig. 1C), consistent with the previous limited reports of introns in *E. histolytica* (25, 34, 40). One of the

unique features of the spliceosomal introns identified in *T. vaginalis* and *G. lamblia* is the incorporation of a well-conserved branch point sequence into an extended 3' splice site (32, 35). Of the known *T. vaginalis* introns, the branch point sequence ACU AAC is incorporated into the extended 3' splice site, prompting speculation that *T. vaginalis* spliceosomes may combine the steps of branch point- and 3'-splice site recognition (38). In contrast, only 90 of the 3,188 predicted *E. histolytica* introns contain this sequence (data not shown), indicating that this branch point sequence is not strictly conserved in *E. histolytica* introns. However, sequences that resemble the degenerate mammalian branch point are found in many *E. histolytica* introns (40). Lastly, a substantial number of *E. histolytica* genes are predicted to contain multiple introns (24), raising the issue of whether some of these genes undergo regulated or alternative splicing.

Comparison of intron predictions with EST splice patterns.

Although 3,188 introns have been predicted in *E. histolytica*, less than 20 have been experimentally validated (25, 33, 40). In order to determine the accuracy of the intron predictions, we directly compared the predicted introns to their spliced counterparts by mining an EST library for hallmarks of splicing. To accommodate the putative intron, we allowed for gaps of ≥ 23 nucleotides to occur in the EST relative to its genome sequence (Fig. 1A). Of the 3,188 predicted intronic loci, 275 are spanned by ESTs that satisfy these criteria and are therefore testable. In order to determine if the predictions matched the ESTs, we compared the EST gap coordinates to those of the predicted intron. One hundred sixty-four of the EST gap coordinates matched the coordinates of the predicted intron, indicating that they are spliced exactly as annotated (see Table S1 in the supplemental material), at splice sites primarily composed of GUUUGU-UAG (Fig. 1D). However, for other introns, the predicted coordinates did not match those deduced from the ESTs, indicating that these predictions are incorrect (Table 1). In general, we noticed that splice sites that were incorrectly predicted to use a splice donor other than the preferred GUUUGU are not used *in vivo*, in favor of a nearby GUUUGU. Likewise, a nearby UAG 3' splice acceptor site appears to be utilized over GAG, AAG, and, in some instances, even a neighboring UAG. Moreover, in nearly all cases, the spliced intron was smaller than predicted. Lastly, although 103 of the 275 testable putative introns contain canonical splice sites, we failed to find evidence for their removal in any of their corresponding ESTs (Fig. 1D; also see Table S2 in the supplemental material). This suggests that either these are not introns, are not spliced under conditions represented in the EST library, or have such low splicing efficiency that no spliced isoforms were cloned.

Mining the ESTs for unannotated introns and genes.

In order to identify novel processing events within the *E. histolytica* EST database, we mined the ESTs for transcripts with intron-like features independent of any prior predictions. We queried the ESTs for regions that have two or more blocks of sequence with at least 98% identity to the genomic sequence and are separated by a gap of 40 to 200 nucleotides and hand collated the data. In total, we identified 35 novel introns, each of which was classified into one of three categories based on how it affected the protein-reading frame (Table 2).

Class I introns. Class I is the largest class of novel introns we identified. These introns are located in or near annotated genes but in regions not annotated to be intronic; i.e., they were predicted to be exonic or in regions immediately proximal to an open reading frame. However, *in silico* translation of the surrounding spliced sequence revealed an extension of the protein-coding region of the adjacent genes.

Class II introns. Class II introns map immediately proximal to annotated open reading frames. However, in contrast to Class I introns, *in silico* translation of the surrounding spliced sequences did not alter the protein-coding region of the adjacent genes, suggesting that these introns reside in their untranslated regions (UTRs). Thus, their retention or removal does not affect the protein-coding potential of the gene.

Class III introns. Class III introns are located in regions currently annotated as "intergenic" and not predicted to have any protein-coding potential. However, *in silico* translation of

the spliced sequences surrounding the introns uncovered several novel proteins with extended reading frames. Most of these predicted genes have not been previously identified in *E. histolytica* but have homologs in other organisms. One of the novel genes (on BLAT scaffold 154) lacks homology to any known proteins and contains two introns (one represented by an EST and the other identified computationally while deciphering the protein-reading frame). Splicing of both introns was confirmed by reverse transcription (RT)-PCR and cDNA sequencing (data not shown).

RT-PCR validation and sequencing of the BLAT intron predictions. In order to experimentally confirm splicing of the novel introns identified above, we performed RT-PCR on cDNA generated from log-phase *E. histolytica* HM-1:IMSS trophozoites grown under standard axenic culture conditions. In all cases tested, PCR amplification of cDNA using exonic primers spanning the novel introns generated a product smaller than that amplified from genomic DNA, consistent in size with that from splicing of the predicted introns from these transcripts (Fig. 2). The cDNAs for acriflavin resistance protein, pantothenate kinase, 47.m00184, 21.m00231, and (154.m), a novel gene with no homology to any known protein in the GenBank database, were cloned and sequenced (data not shown). In all cases, the sequencing results confirmed that the splice sites indicated in Table 2 were used. Given the canonical splice donor and acceptor sequences in Table 2, we expect that these remaining novel introns are likewise correct. These data demonstrate that the novel introns we identified are efficiently spliced in log-phase *E. histolytica* trophozoites and suggest that many additional introns remain to be uncovered.

EST evidence for intron retention and alternate 3'-splice site selection. Multi-intron-containing genes are generally a feature of higher eukaryotes and are often accompanied by alternative splicing, such as exon skipping and mutually exclusive exons (17). Approximately 6% of the presently annotated genes in *E. histolytica* are predicted to be multi-intron containing (24). However, none of the ESTs that span two or more predicted introns in a gene exhibit evidence for exon skipping and mutually exclusive exons (data not shown). Moreover, we found no evidence of exon skipping or mutually exclusive exons in RT-PCR experiments in log-phase *E. histolytica* trophozoites using primers that span several exons in 10 other multi-intron-containing genes (data not shown).

Other forms of alternative splicing, such as intron retention, are more prevalent in lower eukaryotes with fewer multi-intron-containing genes and smaller introns (21). In order to see if there was any evidence in the ESTs for intron retention, we sought to compare the number of spliced ESTs to the number of unspliced ESTs for each of the 164 introns for which there is functional/EST evidence of splicing (see Table S1 in the supplemental material). While 87% of the 164 introns are spliced in 100% of their representative ESTs, 13% are spliced in only a fraction of their representative ESTs. Two possibilities can readily explain this observation: (i) the fraction of "unspliced" ESTs for an individual intron are derived from its pre-mRNAs cloned prior to splicing; or (ii) the fraction of "unspliced" ESTs for an individual intron are derived from a distinct growth condition in which the intron is selectively retained, i.e., intron retention. Additional directed and high-throughput experiments, such as splicing-sensitive microarray

TABLE 2. Novel *E. histolytica* introns culled from the EST data^a

Representative EST	Transcript	GenBank accession no.	Predicted function	5' Splicing site	3' Splicing site	BLAT coordinates	BLAT scaffold	Size	No. of unique ESTs	Effect on protein
Class I										
EHAA254TF	101.m00114	ELA47515.1	Conserved hypothetical protein	GUUUGU	AAG	10427-10489	101	62	1	Alters the C terminus
EHAA741TF	42.m00181	N/A	Pseudogene Ras family GTPase	GUUUGU	UAG	30857-30960	42	103	7	Alters the C terminus
EHA244TR	19.m00316	ELA50600.1	Hypothetical protein	GUUUGU	UAG	77147-77207	19	60	1	Eliminates amino acids
EHAA453TR	178.m00101	ELA45803.1	3' UTR of hypothetical protein	GUUUGU	AAG	36163-36214	178	51	3	Alters the C terminus
EHAA547TR	110.m00129	ELA47260.1	Rho family GTPase	GUUUGU	UAG	38325-38392	110	67	2	Alters the C terminus
EHABP41TR	254.m00073	ELA44597.1	Hypothetical protein	GUUUGU	AAG	5957-6014	254	57	3	Alters the C terminus
EHADQ25TR	18.m00335	ELA50675.1	DNA replication licensing factor	GUUUGU	UAG	98259-98343	18	84	1	Alters the C terminus
EHAET77TR	18.m00328	ELA50668.1	Molybdopterin biosynthesis	GUUUGU	UAG	90251-90312	18	61	2	Alters the C terminus
EHAGK16TR	264.m00090	ELA44495.1	Sec13 protein	GUUUGU	UAG	5564-5620	264	56	3	Alters the N terminus
EHAH331TR	264.m00090	ELA44495.1	Sec13 protein	GUUUGU	UAG	5656-5710	264	54	2	Alters the N terminus
EHAEE26TR	133.m00132	N/A	Hypothetical protein	GUUUGU	UAG	16335-16395	133	60	1	Alters the N and C termini
EHAB255TR	52.m00167	ELA49102.1	Rho family GTPase	GUUUGU	UAG	69361-69424	52	63	5	Alters the C terminus
EHAA702TR	231.m00059	ELA44885.1	Conserved hypothetical protein	GUUUGU	AAG	7731-7834	231	103	8	Alters the N terminus
EHAGH85TR ^b	47.m00184	ELA49297.1	Hypothetical protein	GUUUGU	AAG	70138-70195	47	57	1	Alters the N terminus
EHABT01TR	57.m00155	ELA48912.1	Hypothetical protein	GUUUGU	UAG	34651-34702	57	51	1	Eliminates amino acids
EHAEO44TR	364.m00046	ELA43561.1	60S ribosomal protein L27a	GUUUGU	UAG	15314-15429	364	115	1	Alters the N terminus
EHAET36TR	135.m00095	ELA46630.1	Hypothetical protein	GUUUGU	UAG	9119-9259	135	140	6	Alters the N terminus
EHADY14TR	366.m00044	ELA43555.1	Hypothetical protein	GUUUGU	UAG	6738-6786	366	48	1	Alters the N terminus
EHAG990TR	152.m00113	ELA46298.1	Hypothetical protein	GUUUGU	UAG	24791-24927	152	136	1	Alters the N terminus
EHAAP93TR	195.m00094	ELA45475.1	60S ribosomal protein L24	GUUUGU	UAG	31405-31461	195	56	2	Alters the N terminus
Class II										
EHAA544TR	88.m00175	ELA47893.1	3' UTR of hypothetical protein	GUUUGU	UAG	55917-56020	88	103	2	N/A
EHAEE26TR	23.m00311	ELA50387.1	3' UTR of in Rho GTPase	GUUUGU	UAG	24514-24574	23	60	1	N/A
EHAES83TR	350.m00049	ELA43647.1	5' UTR of in Rho GTPase	GUUUGU	UAG	5995-6143	350	148	1	N/A
EHAA378TR ^b	21.m00231	ELA50513.1	5' UTR of 40S ribosomal protein S14	GUUUGU	UAG	17466-17539	21	73	3	N/A
EHAA726TR	312.m00035	ELA43981.1	5' UTR of 60S ribosomal protein L9	GUUUGU	UAG	6822-6956	312	134	12	N/A
EHAHG49TR	144.m00101	ELA46471.1	Similar to cap binding protein	GUUUGU	UAG	16107-16176	144	69	1	N/A
EHAFO84TR	39.m00252	ELA49583.1	Glycotransferase	GUUUGA	UAG	80547-80602	39	55	1	N/A
Class III										
EHAAM093TR	N/A	N/A	Similar to 6.m000429	GUUUGA	UAG	14120-14172	338	52	1	New to <i>E. histolytica</i>
EHACJ50TR ^b	N/A	N/A	Similar to pantothenate kinase	GUUUGU	AAG	76031-76107	39	76	1	New to <i>E. histolytica</i>
EHAFO09TR	N/A	N/A	Similar to UFDF1-1	GUUUGU	UAG	73812-73859	11	47	1	New to <i>E. histolytica</i>
EHAC353TR ^b	N/A	N/A	Similar to acriflavin resistance protein	GUUUGU	UAG	4398-4451	389	53	2	New to <i>E. histolytica</i>
EHAEL21TR	N/A	N/A	Similar to YIP1 Golgi protein	GUUUGU	UAG	52191-52240	62	49	2	New to <i>E. histolytica</i>
EHAEL30TR	N/A	N/A	CCCH-domain protein	GUUUGU	UAG	89669-89734	5	65	2	New to <i>E. histolytica</i>
EHAC32TR	N/A	N/A	CCCH domain protein	GUUUGU	UAG	90154-90220	5	66	2	New to <i>E. histolytica</i>
EHAHB45TR ^b	N/A	N/A	No homology, novel	GUUUGU	UAG	23491-23547	154	56	1	New to <i>E. histolytica</i>

^a Class I introns align by BLAT to genes that were not annotated to contain an intron in that region. Class II introns align by BLAT to the UTRs of genes. Class III introns align by BLAT to regions that were not annotated to contain genes. N/A, not applicable.

^b EST for which the spliced product has been cloned and sequenced.

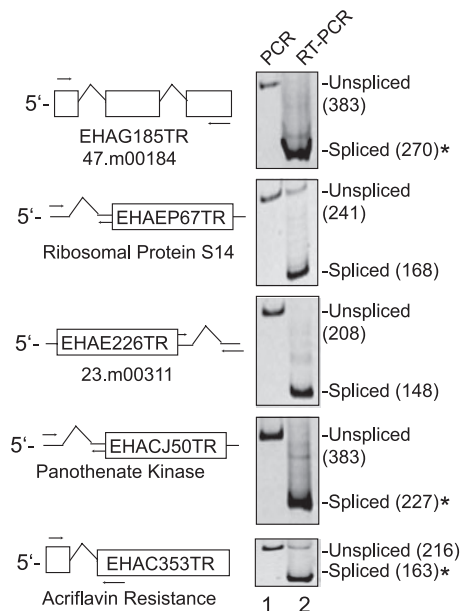


FIG. 2. RT-PCR test of BLAT predictions for *E. histolytica* introns. PCR amplification from either genomic DNA (lane 1) or oligo(dT)-primed cDNA (lane 2) from RNA of log-phase axenic trophozoites for five of the selected novel introns is shown. A diagrammatic gene model is depicted to the left of the gel wherein a box corresponds to an exon. A caret (^) corresponds to an intron. The designations in the boxes beginning with EH and ending with TR are the names of representative ESTs exhibiting the indicated spliced patterns. The common gene name is also indicated below each gene model. Arrows represent the relative positions of the PCR primers. The products were run on a 6% native acrylamide gel and stained with ethidium bromide. The PCR product sizes are indicated in parentheses, and those marked by an asterisk (*) were cloned and sequenced.

(5), and larger cDNA libraries are needed to identify individual processing events and monitor the alterations in processing during parasite growth and development.

Examples of regulated splicing have been described in other systems as a mechanism to turn transcripts on and off (2, 6, 8, 22, 37). Because we have not tested every growth condition in the life of an amoeba, we cannot formally exclude the possibility that the 37% of introns for which we see no evidence of splicing are indeed spliced under a given condition. One point at which alternate isoforms of the same pre-mRNA may be generated is the developmental switch between the trophozoite and cyst forms of *E. histolytica*. Microarray data indicate that ~15% of annotated genes change ± 3 -fold between trophozoites and cysts of *E. histolytica* (12). Whether these changes in RNA abundance between the life cycle stages reflect alterations in transcription frequency or decay as a result of regulated processing remains to be tested.

Finally, some genes are known to generate different proteins as a result of splicing at alternate 5' and 3' splice sites (10, 16). In order to see if there was any evidence in the EST library for alternate 5'- and 3'-splice site usage, we individually mined each spliced intron for examples of ESTs in which all of the coordinates for one of the splice sites was fixed while the other varied. We found no evidence for alternate 5'-splice site usage. However, 89.m00113, a gene with similarity to human Sm_B/B' protein, has representative ESTs in which different 3' splice

sites are used for the penultimate intron, which would introduce two additional amino acids in the C terminus (data not shown). Curiously, the human Sm_B and Sm_{B'} isoforms are derived from alternative splicing using different 3' splice sites of the penultimate intron that are distinguishable by autoantibodies generated in people with systemic lupus erythematosus (19). Thus, overall, we found EST evidence for candidate intron retention and alternative 3'-splice site usage.

***E. histolytica* spliceosomal RNAs (snRNAs).** snRNAs bound in the spliceosomal complex of over 150 proteins interact with the intron through RNA-RNA interactions (18). The pre-mRNA reaction partners for the two catalytic steps of splicing are brought into proximity through dynamic rearrangements of the pre-mRNA/snRNA and snRNA/snRNA complexes requiring U1, U2, U4, U5, and U6 snRNAs (27). To date, U6 is the only *E. histolytica* snRNA that has been identified (28). Given the essential role of the snRNAs in splicing, we queried the *E. histolytica* genome for the presence of the U1, U2, U4, and U5 snRNAs.

U2 snRNA is involved in pre-mRNA/snRNA base pairing and juxtapositioning of the branch point adenosine for the first transesterification reaction. In order to identify the *E. histolytica* U2 snRNA, we downloaded 553 U2 snRNA sequences from Rfam and built an HMM to look for conserved features. The region on scaffold 25 from 23993 to 24173 had the greatest similarity to known U2 snRNAs and was selected for Northern blot analysis. We saw U2 accumulate as a predominate species, 178 nucleotides in length, in trophozoite RNA (Fig. 3C). Its putative secondary structure is similar to those of other known U2 snRNAs, including the branch point binding sequence and the Sm binding site (data not shown), and is predicted to interact with U6 snRNA in the conserved fashion. The U4 snRNA base pairs with U6 snRNA, acting as its chaperone and maintaining it in an unfolded conformation while part of the U4/U5/U6 tri-snRNP (13). We applied the above approach to identify U4 snRNA based on the 372 U4 snRNA sequences in Rfam. We identified the region on scaffold 150 from 39898 to 40028. Subsequent Northern blot analysis of this region uncovered a predominant band 125 nucleotides in length (Fig. 3C). This putative U4 snRNA is able to interact with the previously identified U6 snRNA in a conserved fashion. Of note, the U4 snRNA also seems to lack the terminal 3' stem loop found in higher eukaryotes (30).

U5 snRNA interacts with the exons upstream of the 5' splice site and downstream of the 3' splice site, tethering them in the active site for the second transesterification (31). Our efforts to identify the *E. histolytica* U5 snRNA using the above means failed. Therefore, we used BLAT for each of the 235 U5 sequences in the Rfam database against the *E. histolytica* genome scaffolds. We identified a region on scaffold 283 from 9300 to 9468 with significant homology to the U5 sequences from *Entosiphon sulcatum*, *Oryza sativa*, *Zea mays*, and *Arabidopsis thaliana*. Northern blot analysis of this region uncovered a single band 118 nucleotides in length (Fig. 3C). Secondary structure prediction showed its potential to form the evolutionarily conserved site in stems I and II as well as the Sm binding site (Fig. 3B). Using the computational approaches outlined above, we were unable to identify U1. Whether this indicates that the *E. histolytica* U1 sequence is substantially

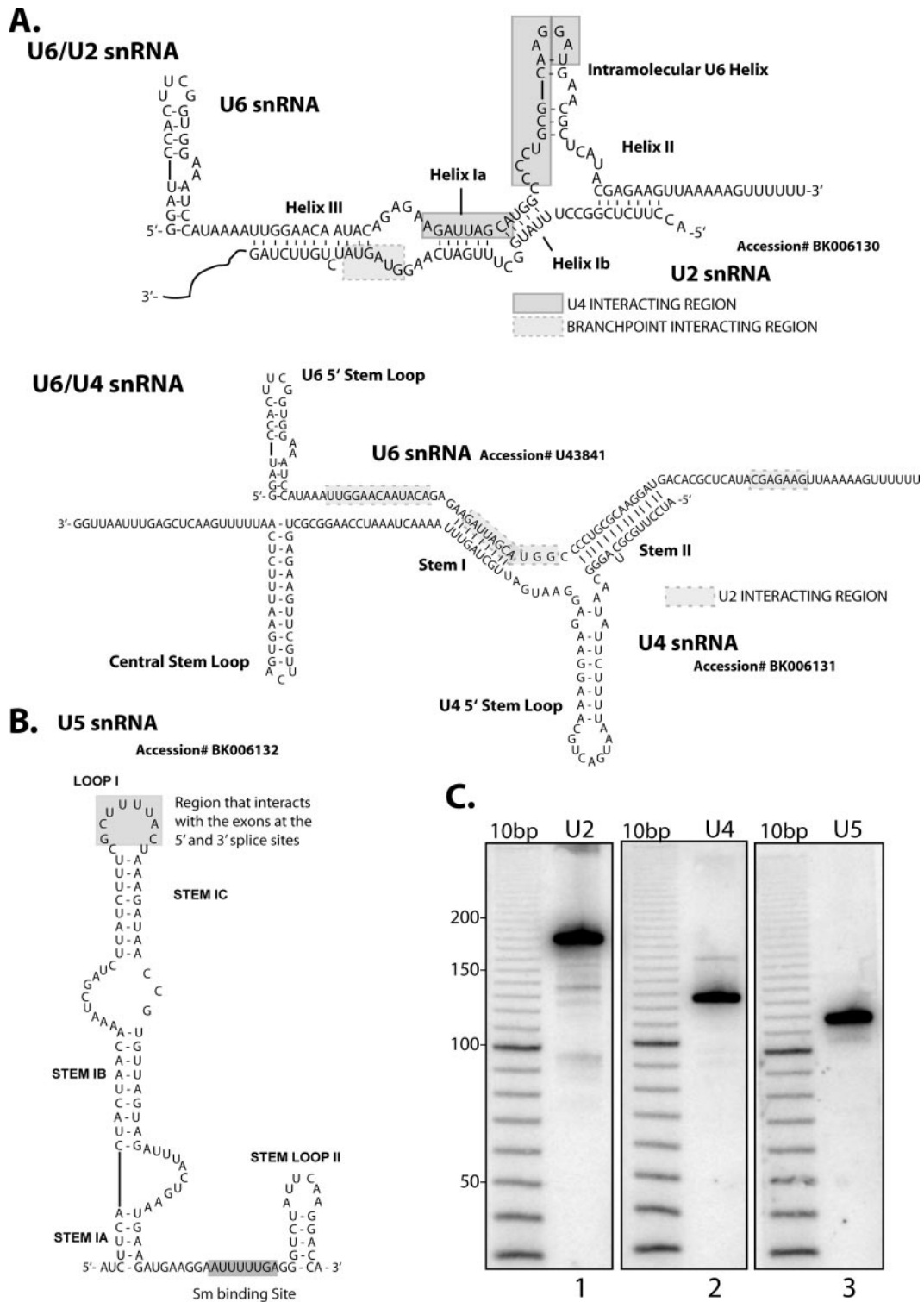


FIG. 3. *E. histolytica* spliceosomal RNAs (snRNAs). (A) Predicted secondary structures of U2 snRNA bound to U6 snRNA and U4 snRNA bound to U6 snRNA. (B) Predicted secondary structure of U5 snRNA. (C) Northern blots for U2, U4, and U5 snRNAs. Ten micrograms of HM-1:IMSS total RNA was fractionated on a 6% denaturing acrylamide gel and probed with a radiolabeled oligo targeting each of the predicted snRNAs. A radiolabeled 10-base-pair marker (Invitrogen) was loaded in parallel to assess the sizes of each of the snRNAs.

different or that it has escaped being sequenced is not clear at present.

Conclusions. Despite the ability of RNA processing to markedly alter the coding potential of genes, the mechanisms that control these events in *E. histolytica* are poorly understood. We compared the splice patterns mined from EST data to 275 computational intron predictions. We found evidence supporting the splicing of 60% of introns exactly as predicted. Additionally, we identified several splice site misannotations, novel introns in annotated genes, and novel intron-containing genes. Since the EST data we analyzed represented ~7% of the predicted amoebic genes, our work indicates that a larger-scale EST library would significantly improve gene annotation and uncover additional useful information regarding mechanisms of RNA processing in *E. histolytica*. This work represents the first large-scale test of splicing in a deep-branching eukaryote and indicates that similar analyses in other systems may be similarly fruitful.

ACKNOWLEDGMENTS

We thank all members of the Singh lab, specifically Gretchen Ehrenkauf and Jason Hackney, for critical and editorial comments on the manuscript; Neil Hall and Lis Caler (TIGR) for providing the EST sequences and incorporating data into genome reannotation; Barbara Mann (University of Virginia) for providing information on the EST library; and Neha Gupta for preliminary RT-PCR analysis of intron-containing genes.

This work was supported by NIH grants AI-053724 to Upinder Singh and T32 AI-07502 to Carrie A. Davis.

REFERENCES

- Ali, I. K., M. Zaki, and C. G. Clark. 2005. Use of PCR amplification of tRNA gene-linked short tandem repeats for genotyping *Entamoeba histolytica*. *J. Clin. Microbiol.* **43**:5842–5847.
- Averbeck, N., S. Sunder, N. Sample, J. A. Wise, and J. Leatherwood. 2005. Negative control contributes to an extensive program of meiotic splicing in fission yeast. *Mol. Cell* **18**:491–498.
- Bateman, A., E. Birney, R. Durbin, S. R. Eddy, R. D. Finn, and E. L. Sonnhammer. 1999. Pfam 3.1: 1313 multiple alignments and profile HMMs match the majority of proteins. *Nucleic Acids Res.* **27**:260–262.
- Carlton, J. M., R. P. Hirt, J. C. Silva, A. L. Delcher, M. Schatz, Q. Zhao, J. R. Wortman, S. L. Bidwell, U. C. Alsmark, S. Besteiro, T. Sicheritz-Ponten, C. J. Noel, J. B. Dacks, P. G. Foster, C. Simillion, Y. Van de Peer, D. Miranda-Saavedra, G. J. Barton, G. D. Westrop, S. Muller, D. Dessi, P. L. Fiori, Q. Ren, I. Paulsen, H. Zhang, F. D. Bastida-Corcuera, A. Simoes-Barbosa, M. T. Brown, R. D. Hayes, M. Mukherjee, C. Y. Okumura, R. Schneider, A. J. Smith, S. Vanacova, M. Villalvazo, B. J. Haas, M. Pertea, T. V. Feldblyum, T. R. Utterback, C. L. Shu, K. Osoegawa, P. J. de Jong, I. Hrdy, L. Horvathova, Z. Zubacova, P. Dolezal, S. B. Malik, J. M. Logsdon, Jr., K. Henze, A. Gupta, C. C. Wang, R. L. Dunne, J. A. Upercroft, P. Upercroft, O. White, S. L. Salzberg, P. Tang, C. H. Chiu, Y. S. Lee, T. M. Embley, G. H. Coombs, J. C. Mottram, J. Tachezy, C. M. Fraser-Liggett, and P. J. Johnson. 2007. Draft genome sequence of the sexually transmitted pathogen *Trichomonas vaginalis*. *Science* **315**:207–212.
- Clark, T. A., C. W. Sugnet, and M. Ares, Jr. 2002. Genomewide analysis of mRNA processing in yeast using splicing-specific microarrays. *Science* **296**:907–910.
- Dabeva, M. D., M. A. Post-Beittenmiller, and J. R. Warner. 1986. Autogenous regulation of splicing of the transcript of a yeast ribosomal protein gene. *Proc. Natl. Acad. Sci. USA* **83**:5854–5857.
- Davis, C. A., and M. Ares, Jr. 2006. Accumulation of unstable promoter-associated transcripts upon loss of the nuclear exosome subunit Rrp6p in *Saccharomyces cerevisiae*. *Proc. Natl. Acad. Sci. USA* **103**:3262–3267.
- Davis, C. A., L. Grate, M. Spingola, and M. Ares, Jr. 2000. Test of intron predictions reveals novel splice sites, alternatively spliced mRNAs and new introns in meiotically regulated genes of yeast. *Nucleic Acids Res.* **28**:1700–1706.
- Diamond, L. S., C. G. Clark, and C. C. Cunnick. 1995. YI-S, a casein-free medium for axenic cultivation of *Entamoeba histolytica*, related *Entamoeba*, *Giardia intestinalis* and *Trichomonas vaginalis*. *J. Eukaryot. Microbiol.* **42**:277–278.
- Dou, Y., K. L. Fox-Walsh, P. F. Baldi, and K. J. Hertel. 2006. Genomic splice-site analysis reveals frequent alternative splicing close to the dominant splice site. *RNA (New York)* **12**:2047–2056.
- Eddy, S. R., and R. Durbin. 1994. RNA sequence analysis using covariance models. *Nucleic Acids Res.* **22**:2079–2088.
- Ehrenkauf, G. M., R. Haque, J. A. Hackney, D. J. Eichinger, and U. Singh. 2007. Identification of developmentally regulated genes in *Entamoeba histolytica*: insights into mechanisms of stage conversion in a protozoan parasite. *Cell. Microbiol.*
- Gmeiner, W. H. 2002. The structure and dynamics of the U4/U6 snRNP: implications for pre-mRNA splicing and use as a model system to investigate the RNA-mediated effects of (5F)Ura. *J. Biomol. Struct. Dyn.* **19**:853–862.
- Griffiths-Jones, S., A. Bateman, M. Marshall, A. Khanna, and S. R. Eddy. 2003. Rfam: an RNA family database. *Nucleic Acids Res.* **31**:439–441.
- Griffiths-Jones, S., S. Moxon, M. Marshall, A. Khanna, S. R. Eddy, and A. Bateman. 2005. Rfam: annotating non-coding RNAs in complete genomes. *Nucleic Acids Res.* **33**:D121–124.
- Hiller, M., K. Huse, K. Szafranski, N. Jahn, J. Hampe, S. Schreiber, R. Backofen, and M. Platzer. 2004. Widespread occurrence of alternative splicing at NAGNAG acceptors contributes to proteome plasticity. *Nat. Genet.* **36**:1255–1257.
- Johnson, J. M., J. Castle, P. Garrett-Engele, Z. Kan, P. M. Loerch, C. D. Armour, R. Santos, E. E. Schadt, R. Stoughton, and D. D. Shoemaker. 2003. Genome-wide survey of human alternative pre-mRNA splicing with exon junction microarrays. *Science* **302**:2141–2144.
- Jurica, M. S., and M. J. Moore. 2003. Pre-mRNA splicing: awash in a sea of proteins. *Mol. Cell* **12**:5–14.
- Kaufman, K. M., M. Y. Kirby, M. T. McClain, J. B. Harley, and J. A. James. 2001. Lupus autoantibodies recognize the product of an alternative open reading frame of SmB/B'. *Biochem. Biophys. Res. Commun.* **285**:1206–1212.
- Kent, W. J. 2002. BLAT—the BLAST-like alignment tool. *Genome Res.* **12**:656–664.
- Kim, E., A. Magen, and G. Ast. 2007. Different levels of alternative splicing among eukaryotes. *Nucleic Acids Res.* **35**:125–131.
- Kishida, M., T. Nagai, Y. Nakaseko, and C. Shimoda. 1994. Meiosis-dependent mRNA splicing of the fission yeast *Schizosaccharomyces pombe* mes1⁺ gene. *Curr. Genet.* **25**:497–503.
- Krogh, A., M. Brown, I. S. Mian, K. Sjolander, and D. Haussler. 1994. Hidden Markov models in computational biology. Applications to protein modeling. *J. Mol. Biol.* **235**:1501–1531.
- Loftus, B., I. Anderson, R. Davies, U. C. Alsmark, J. Samuelson, P. Amedeo, P. Roncaglia, M. Berriman, R. P. Hirt, B. J. Mann, T. Nozaki, B. Suh, M. Pop, M. Duchene, J. Ackers, E. Tannich, M. Leippe, M. Hofer, I. Bruchhaus, U. Willhoelt, A. Bhattacharya, T. Chillingworth, C. Churcher, Z. Hance, B. Harris, D. Harris, K. Jagels, S. Moule, K. Mungall, D. Ormond, R. Squares, S. Whitehead, M. A. Quail, E. Rabinovitch, H. Norbertczak, C. Price, Z. Wang, N. Guillen, C. Gilchrist, S. E. Stroup, S. Bhattacharya, A. Lohia, P. G. Foster, T. Sicheritz-Ponten, C. Weber, U. Singh, C. Mukherjee, N. M. El-Sayed, W. A. Petri, Jr., C. G. Clark, T. M. Embley, B. Barrell, C. M. Fraser, and N. Hall. 2005. The genome of the protist parasite *Entamoeba histolytica*. *Nature* **433**:865–868.
- Lohia, A., and J. Samuelson. 1993. Cloning of the Eh cdc2 gene from *Entamoeba histolytica* encoding a protein kinase p34cdc2 homologue. *Gene* **127**:203–207.
- MacFarlane, R. C., and U. Singh. 2006. Identification of differentially expressed genes in virulent and nonvirulent *Entamoeba* species: potential implications for amebic pathogenesis. *Infect. Immun.* **74**:340–351.
- Madhani, H. D., and C. Guthrie. 1994. Dynamic RNA-RNA interactions in the spliceosome. *Annu. Rev. Genet.* **28**:1–26.
- Miranda, R., L. M. Salgado, R. Sanchez-Lopez, A. Alagon, and P. M. Lizardi. 1996. Identification and analysis of the u6 small nuclear RNA gene from *Entamoeba histolytica*. *Gene* **180**:37–42.
- Mourier, T., and D. C. Jeffares. 2003. Eukaryotic intron loss. *Science* **300**:1393.
- Myslinski, E., and C. Branlant. 1991. A phylogenetic study of U4 snRNA reveals the existence of an evolutionarily conserved secondary structure corresponding to 'free' U4 snRNA. *Biochimie* **73**:17–28.
- Newman, A. J., and C. Norman. 1992. U5 snRNA interacts with exon sequences at 5' and 3' splice sites. *Cell* **68**:743–754.
- Nixon, J. E., A. Wang, H. G. Morrison, A. G. McArthur, M. L. Sogin, B. J. Loftus, and J. Samuelson. 2002. A spliceosomal intron in *Giardia lamblia*. *Proc. Natl. Acad. Sci. USA* **99**:3701–3705.
- Plaimauer, B., S. Ortner, G. Wiedermann, O. Scheiner, and M. Duchene. 1994. An intron-containing gene coding for a novel 39-kilodalton antigen of *Entamoeba histolytica*. *Mol. Biochem. Parasitol.* **66**:181–185.
- Roy, S. W., M. Irimia, and D. Penny. 2006. Very little intron gain in *Entamoeba histolytica* genes laterally transferred from prokaryotes. *Mol. Biol. Evol.* **23**:1824–1827.
- Russell, A. G., T. E. Shutt, R. F. Watkins, and M. W. Gray. 2005. An ancient spliceosomal intron in the ribosomal protein L7a gene (Rpl7a) of *Giardia lamblia*. *BMC Evol. Biol.* **5**:45.
- Sakakibara, Y., M. Brown, R. Hughey, I. S. Mian, K. Sjolander, R. C.

- Underwood, and D. Haussler. 1994. Stochastic context-free grammars for tRNA modeling. *Nucleic Acids Res.* **22**:5112–5120.
37. Spingola, M., and M. Ares, Jr. 2000. A yeast intronic splicing enhancer and Nam8p are required for Mer1p-activated splicing. *Mol. Cell* **6**:329–338.
38. Vanáčová, S., W. Yan, J. M. Carlton, and P. J. Johnson. 2005. Spliceosomal introns in the deep-branching eukaryote *Trichomonas vaginalis*. *Proc. Natl. Acad. Sci. USA* **102**:4430–4435.
39. Vogel, G. 2006. Infectious diseases. Tackling neglected diseases could offer more bang for the buck. *Science* **311**:592–593.
40. Wilihoef, U., E. Campos-Gongora, S. Touzni, I. Bruchhaus, and E. Tannich. 2001. Introns of *Entamoeba histolytica* and *Entamoeba dispar*. *Protist* **152**: 149–156.
41. World Health Organization. 1997. A consultation with experts on amoebiasis. WHO/PAHO/UNESCO report. Mexico City, Mexico, 28–29 January, 1997. *Epidemiol. Bull.* **18**:13–14.
42. Yamauchi, K., T. Ochiai, and I. Usuki. 1992. The unique structure of the *Paramecium caudatum* hemoglobin gene: the presence of one intron in the middle of the coding region. *Biochim. Biophys. Acta* **1171**:81–87.